Aerosol Science and Technology
Publication details, including instructions for authors and subscription information:
http://www.tandfonline.com/loi/uast20

Long-Term Measurements of Equilibrium Factor and Unattached Fraction of Short-Lived Radon Decay Products in a Dwelling - Comparison with Praddo Model

C. Huet , G. Tymen & D. Boulaud
Published online: 30 Nov 2010.

To cite this article: C. Huet , G. Tymen & D. Boulaud (2001) Long-Term Measurements of Equilibrium Factor and Unattached Fraction of Short-Lived Radon Decay Products in a Dwelling - Comparison with Praddo Model, Aerosol Science and Technology, 35:1, 553-563

To link to this article: http://dx.doi.org/10.1080/02786820117956

Aerosol Science and Technology 35: 553–563 (2001)

Published by Taylor and Francis
0278-6826/01/$12.00 + .00

Long-Term Measurements of Equilibrium Factor and Unattached Fraction of Short-Lived Radon Decay Products in a Dwelling—Comparison with Praddo Model

C. Huet,[1] G. Tymen,[1] and D. Boulaud[2]

[1]*Laboratoire de Recherches Appliquées Atmosphère-Hydrosphère, Université de Bretagne Occidentale, Brest Cedex, France*

[2]*Service d'Etudes et de Recherches en Aérocontamination et en Confinement, Institut de Protection et de Sûreté Nucléaire, Gif-sur-Yvette Cedex, France*

According to the United Nations Scientific Committee on the Effects of Atomic Radiation (UNSCEAR 1993), the dose due to the inhalation of radon decay products represents almost 50% of the total natural radiation dose to the general population. The scientific community is interested in the assessment of the risk induced by domestic radon exposure. The dosimetric models used to estimate the dose are very sensitive to unattached fraction and size distributions, which makes the characterization of the indoor radon decay products aerosol necessary. For this purpose, long-term measurements of unattached fraction (f_p) and equilibrium factor (F) were taken in a dwelling under typical indoor domestic aerosol conditions. An original device consisting of an annular diffusion channel set in parallel with an open filter was developed and calibrated to continuously measure the unattached fraction. Moreover, radon activity concentration and particle concentration were simultaneously monitored. With aged aerosol, particle concentration was found to be very low (between 500 and 5000 cm^{-3}), radon activity concentration ranged from 240 to 2800 Bq m^{-3}, and the mean values of f_p and F were, respectively, 0.31 (0.08–0.67) and 0.16 (0.04–0.45). With aerosol sources, the high increase in particle concentration led to a negligible unattached fraction and raised the equilibrium factor. A correlation relationship was determined between these two parameters under different aerosol conditions. Finally, our experimental results were compared to results obtained with the PRADDO model; this comparison showed a good agreement between these two different approaches.

INTRODUCTION

^{222}Rn is a noble, natural, and radioactive gas present at different concentrations in soils and building materials. After exhalation, it decays into a series of solid short-lived decay products, ^{218}Po, ^{214}Pb, ^{214}Bi, and ^{214}Po. According to the United Nations Scientific Committee on the Effects of Atomic Radiation (UNSCEAR 1993), the dose due to inhalation of radon decay products represents almost 50% of the total natural radiation dose to the general population. An association between an excess risk of lung cancer and exposure to radon and its decay products has been demonstrated in uranium miners and other miners (Lubin et al. 1994). The risk related to indoor domestic exposure has been estimated from the risk projection from underground miners data in association with measurements of indoor radon concentrations. However, exposure conditions in mines generally differ from those in dwellings, and thus the role of radon domestic exposure in the occurrence of lung cancer remains unclear.

The last European program, RARAD (1996–1999), was aimed at assessing the risk induced by inhalation of short-lived radon decay products under genuine living conditions. For this purpose, a multidisciplinary approach was chosen, and the studies addressed five main topics: radioactive aerosol, modeling, humans, animals, and retrospective assessment of radon exposure. As part of the aerosol group, our objective was to determine the properties and behavior of the radon decay products under typical domestic conditions and to focus especially on the temporal variability of unattached fraction and equilibrium factor. As a matter of fact, a sensitivity analysis performed by Marsh and Birchall (1998) using the RADEP model (Birchall and James 1994) showed that the physical parameter that most affected the weighted committed equivalent dose to lung per unit exposure is the unattached fraction.

Our aim required us to first develop a device able to continuously determine the unattached fraction and equilibrium factor over long-term periods. So the annular diffusion channel technique, which avoids the drawbacks of the screen

Received 1 November 1999; accepted 10 April 2000.

Address correspondence to G. Tymen, Laboratoire de Recherches Appliquées Atmosphère-Hydrosphère, Université de Bretagne Occidentale, 6 avenue Le Gorgeu, 29285 Brest Cedex, France. E-mail: georges.tymen@univ-brest.fr

technique, was implemented from May 1997 to April 1998 in a typical house in Brittany, France. This French area is characterized by a granitic subsoil; moreover, in some locations, like the Northwest of Brest, houses with high indoor radon levels are frequent. This is why the investigated dwelling seemed to us a representative place to investigate the unattached fraction, equilibrium factor, and size distributions of attached and unattached radon decay products under realistic living conditions (natural aerosol, cooking, cigar smoke, burning candles, etc.).

Since long-term measurements are time-consuming and expensive, it was also of high interest to compare our experimental data to that obtained with modeling in order to find an alternative to experiments for characterizing the radon exposure of the general population.

The present report will first deal with the original system designed in our laboratory to continuously measure the unattached fraction and equilibrium factor, then we will introduce the results recorded for these two parameters over the long-term measurements performed under different indoor domestic conditions. Finally, our experimental results, especially those about the nanometer radon decay products, will be compared to the results obtained with the PRADDO model (Gouronnec 1995; Gouronnec et al. 1996).

MATERIALS AND METHODS

Radon Activity Concentration Measurement Technique

To continuously measure the radon activity concentration in the air, we designed a system based on electroprecipitation of the positively charged $^{218}Po^{+}$ ions on a surface barrier detector (PIPS Canberra 1700) carried out in a 9 kV electric field. The air was first filtered to remove radon decay products, then continuously sucked into a 0.035 m^3 cylinder made of aluminium. The alpha detector was isolated from the cylinder armature by a piece of Teflon. The $^{218}Po^{+}$ ions formed consequently to the disintegration of radon in the cylinder were then precipitated on the alpha detector because of the electric field applied between the cylinder armature and the alpha detector. The electronic card converting alpha counts into voltage pulses had been designed to only detect the alpha particles emitted with an energy range between 5 and 6 MeV, which permitted us to only detect the alpha particles produced by the decay of $^{218}Po^{+}$. Radon activity concentration was directly proportional to the alpha counts and was determined every 10 min. Data acquisition was completely controlled by a PC. Because of the lack of available radon standard at the time of our study, the responses of different devices had to be compared to calibrate them; so our device was compared to an Alphaguard (Genrich 1994) based on the principle of the ionization chamber. The results recorded at different radon activity concentrations are depicted in Figure 1, which permitted us to determine a conversion factor from alpha pulses to radon activity concentration of 1.127 Bq m^{-3}.

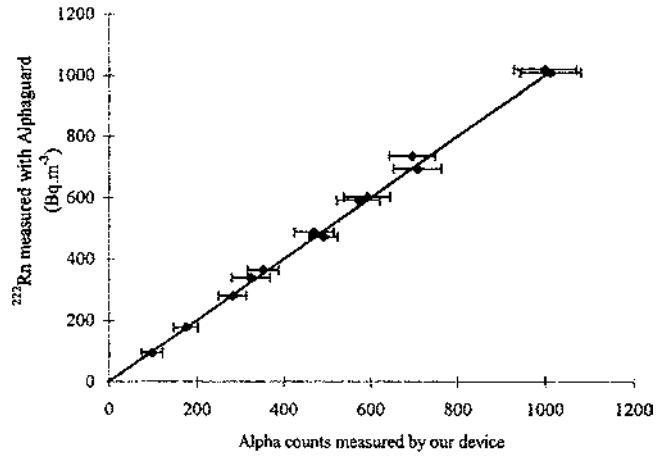

Figure 1. Alpha counts detected by our device versus ^{222}Rn activity concentration measured by an Alphaguard.

Annular Diffusion Channel

Most of the devices usually used to measure the unattached fraction of radon decay products are based on screen techniques. They have allowed one to get good quality information on the potential alpha energy concentration (PAEC) of unattached radon decay products (James et al. 1972; Stranden and Berteig 1982; Reineking et al. 1990; Cheng et al. 1997). Unfortunately, screen techniques have two major drawbacks. These screens may collect some attached radon decay products, which consequently overestimates the activity concentration of unattached radon decay products. Then a correction factor is needed (Reineking et al. 1990). Moreover, some authors have noticed losses due to the recoil of radon decay products collected on the screen (Knutson and George 1994). Therefore a technique previously developed in our laboratory for a specific application, i.e., the annular diffusion channel (ADC) (Kerouanton 1996; Tymen et al. 1999), was improved to permit continuous measurements of the unattached fraction.

Kerouanton et al. (1996) studied by analytical computation the diffusional behavior of ADC geometry; this showed that the annular diffusion channel has almost the same collection efficiency as a flat rectangular channel of equivalent dimensions, considered as the most selective geometry. In the previous application, the ADC was equipped with a LR115 alpha track detector and calibrated in a radon chamber; it was used for the measurement of the nanometer ^{218}Po activity concentration and size distribution averaged over time periods of several weeks in the environment (Tymen et al. 1999). We therefore designed a system composed of two parallel sampling lines. The first one consisted of an ADC equipped downstream with a very high-efficiency membrane filter (Poretics, 0.45 μm). An alpha PIPS detector (Canberra 900) was inserted on the rear part of the internal cylinder, the sensitive surface facing the filter (Figure 2). The size parameters of our system were governed by the following two criteria: the establishment length of the flow had to be as short as possible and the cut-off diameter had to allow the

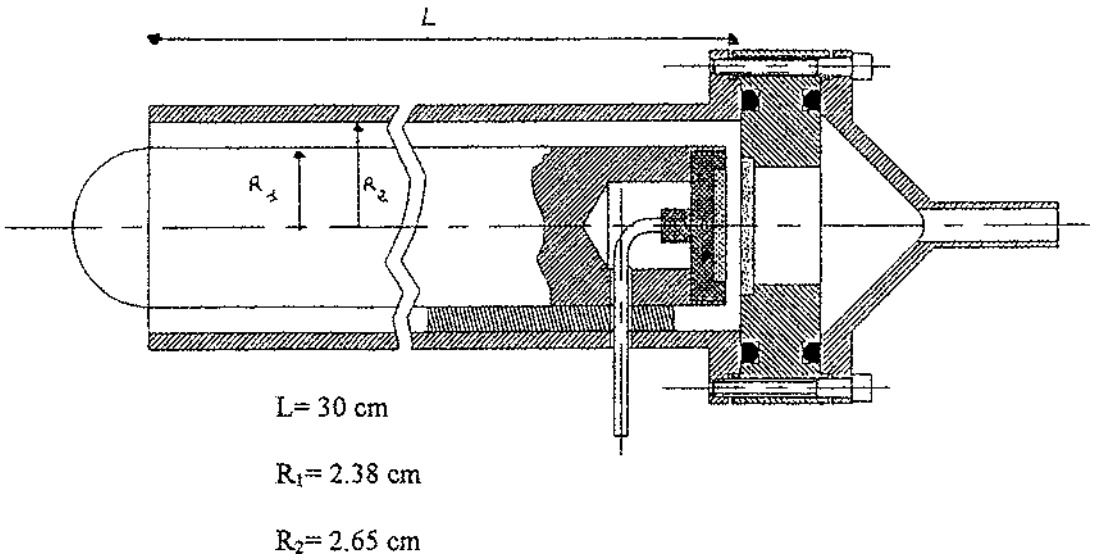

Figure 2. Annular diffusion channel equipped with an alpha detector.

separation of the unattached fraction from the attached one. With the dimensions given in Figure 2 and a flow rate of 7 l min^{-1}, the ADC had a cut-off diameter of 3.2 nm, which was close to the cut-off diameter recommended by Ramamurthi and Hopke (1989), i.e., 4 nm, to optimize the collection of the unattached fraction. The unattached fraction was then deposited by diffusion on the walls of the ADC, whereas the attached radon decay products were collected on the downstream filter facing the alpha detector. The second sampling line consisted of a reference filter equipped with an alpha detector (PIPS Canberra 900) facing a very high-efficiency membrane filter (Poretics, 0.45 μm). The flow rate through the reference filter was set to 20 l min^{-1}. As our reference filter had been designed to let the air pass through a slot between the detector and membrane filter, some aerosol particles could have been removed from the air stream, which thus required us to estimate the inlet losses. So the diffusion losses were first estimated using the formula given by Mercer and Mercer (1970), and second our reference filter was compared with a classical open-face filter of the same characteristics (diameter, flow rate) under different conditions (particle concentration and radon activity concentration). The difference between the two devices was of the order of the counting statistics uncertainty, which thus made us sure that we collected the total radon decay products.

In order to improve the system detection, we developed an expression of the geometric efficiency applicable to different filter-detector configurations. For a distance of 5 mm between the filter and detector, the geometric efficiency calculated according to our expression and verified with a standard source of ^{241}Am was equal to 24% for the two sampling lines. Moreover, energy losses of 6 and 7.7 MeV alpha particles were determined as a function of their path in the air; it showed that for a 5 mm filter-detector distance, only the 7.7 MeV particles emitted between 79.5 and 81.5° from the perpendicular of the filter surface could be counted in the ^{218}Po energy peak. The filter-detector distance was then set to 5 mm, which allowed an optimum geometric efficiency while minimizing the overlap of the two energy peaks.

The two alpha detectors were connected to a PC via two preamplifiers and two amplifiers (Canberra 2012). A program was written for both the acquisition of the alpha spectrum and the pump control so that the sampling and counting procedure was completely controlled by the computer and the measurements were performed every 3 h. In such a case, the previous cycles do not exert any influence on the cycle in progress. The experimental set up used is depicted in Figure 3. The attached and total radon decay products activity concentrations were determined by alpha spectroscopy using the method of Tremblay et al. (1979) according to the following sequence: 0–15 min sampling, a first 0–15 min counting sequence, and a second 20–75 min counting sequence. The way our device had been designed permitted us to simultaneously sample and count, which improved accuracy on the calculated activity concentrations. In order to validate our device, it was compared to a screen technique throughout an intercomparison campaign conducted in a radon chamber (Huet 1999; CEC Report 1998).

Aerosol Measurements

During the experiments, particle concentration was continuously measured using a diffusion battery TSI 3040 associated with a condensation particle counter, TSI 3022A. The diffusion battery was composed of 11 stages. The particle concentration was only measured after 0, 1, 6, 15, 28, and 55 screens. The flow rate through the diffusion battery was 4 l min^{-1}. Knowing the kernel matrix of the diffusion battery and the particle concentration at the outlet of the six stages previously mentioned permitted us to reconstruct the number size distribution of the ambient aerosol using the EVE algorithm (Paatero 1990; Tapper 1995).

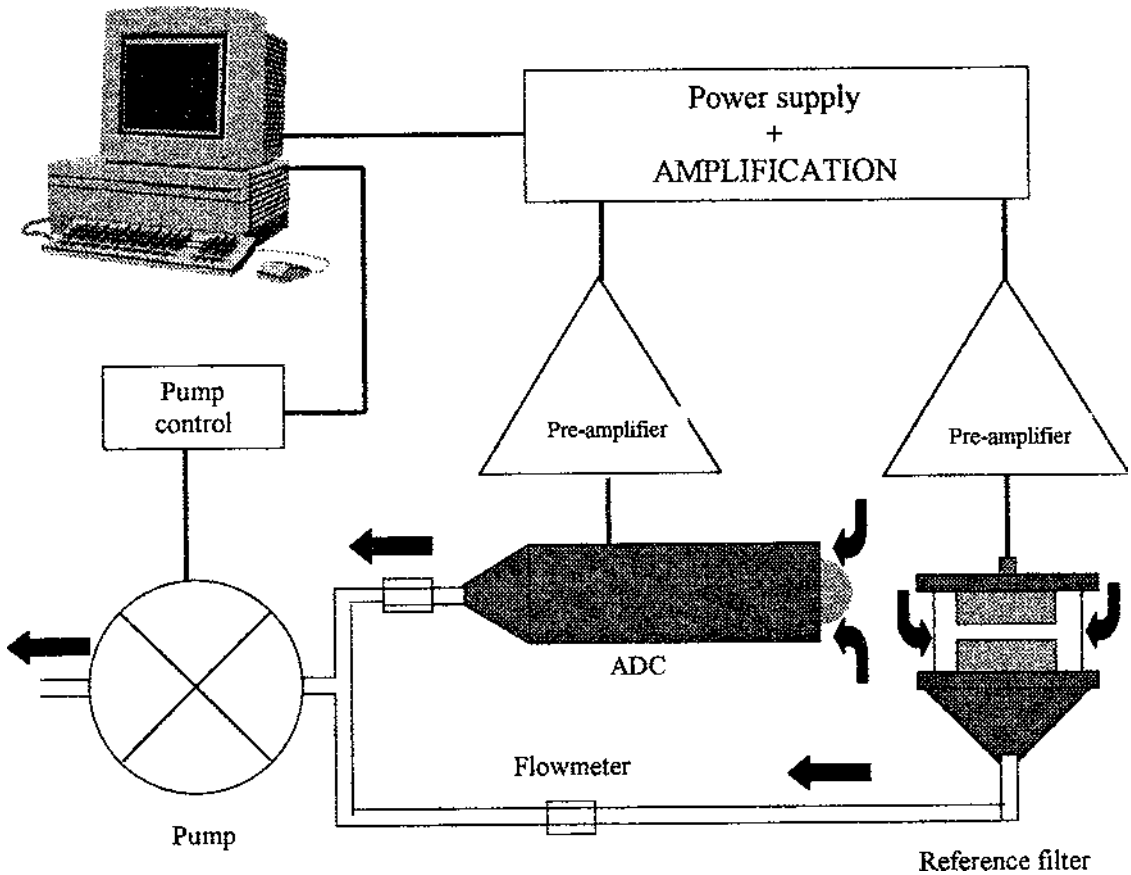

Figure 3. Schematic diagram of our continuous system.

Air Exchange Rate

Radon exhalation and the ventilation rate of a room can be derived from both the increase of the radon concentration by the radon exhalation and the steady-state condition between exhalation and air exchange with the free atmosphere as described by Porstendörfer et al. (1980). Once the room has been ventilated, the increase of radon concentration can be written as

$$c_0^i(t) = \frac{E}{v}(1 - e^{-vt}) + c_0^a, \qquad [1]$$

where is c_0^i the indoor radon concentration, c_0^a is the outdoor radon concentration, E is the exhalation rate (Bq m^{-3} h^{-1}), and v is the ventilation rate (h^{-1}). When $t < 1/v$, the radon emanation is given by

$$E = \frac{\Delta c_0^i(t)}{\Delta t}. \qquad [2]$$

Considering a steady-state condition in the room, the ventilation rate can be determined using

$$v = \frac{\left(E - \lambda_0 c_0^i(\infty)\right)}{\left(c_0^i(\infty) - c_0^a\right)}, \qquad [3]$$

where $c_0^i(\infty)$ is the constant activity concentration and λ_0 is the decay constant for radon.

RESULTS

The house where our measurements were carried out consisted of a ground floor and a first floor; it was equipped with electric heating. Our experimental apparatus was placed in the 67 m^3 furnished living room (ground floor) whose surface-to-volume ratio was about 1.95 m^{-1}. This room had two large windows and a door opening directly to a corridor.

Air Exchange Rate

The air exchange rate was determined according to the procedure described above. Figure 4 depicts a typical example of the growth of radon activity concentration as a function of time after ventilation of the room. The slope of this curve gave us an exhalation rate around 150 Bq m^{-3} h^{-1}, corresponding to an air exchange rate of 0.15 h^{-1}. Additional measurements were carried out and allowed us to determine that the air exchange rate was within 0.1 and 0.4 h^{-1} for a mean value of 0.25 h^{-1}. Although these results are in agreement with the range of values (between 0.1 and 2 h^{-1}) reported in the literature (Grot and Clark 1981; Grimsrud et al. 1983; Knutson 1988), the ventilation rate in this room can be considered low.

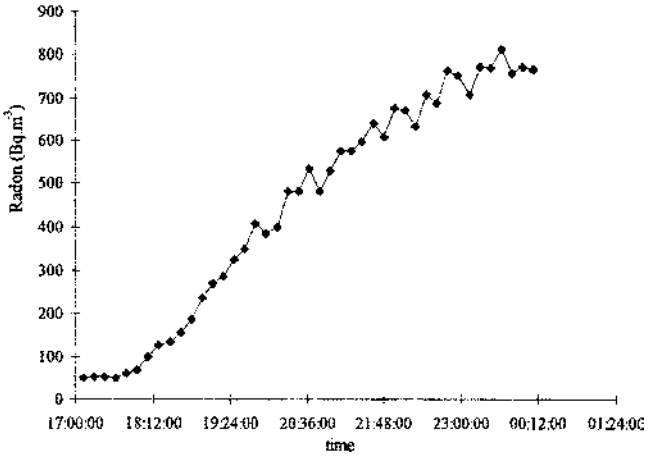

Figure 4. Increase of ^{222}Rn activity concentration versus time after ventilation.

Radon and Particle Concentrations, Ambient Conditions

Throughout the 12 month measurements, we noticed that the room temperature remained stable at 20°C and the relative humidity around 50%; these two parameters were both measured with a Pt probe (SOLOMAT Ltd). All throughtout the year, we observed variations of radon activity concentration within 240 and 2800 Bq m^{-3} with a mean value of 1420 Bq m^{-3}. They were induced by changes in atmospheric conditions. As a matter of fact, low radon activity concentrations were observed during rainy and windy periods. Figure 5 illustrates the variations of radon activity concentration and atmospheric pressure recorded over a 5 day period. It clearly shows that high activity concentrations were obtained under high pressure conditions, i.e., with an anticyclonic weather, whereas radon activity concentration decreased with the arrival of a depression, usually accompanied in Brittany with rain and wind. The decrease of radon activity

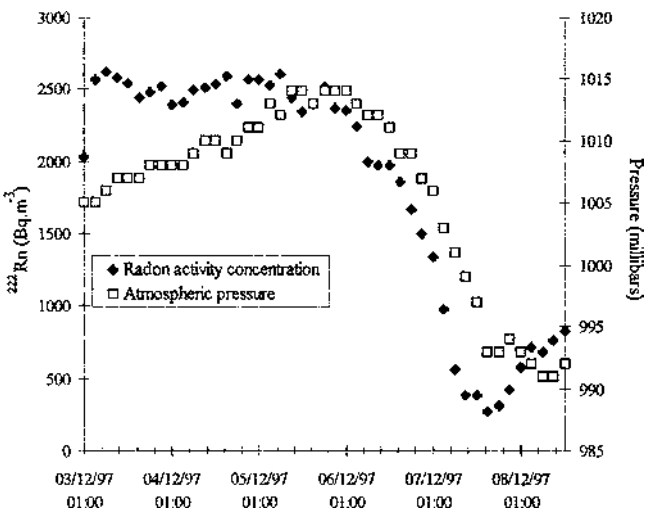

Figure 5. Variations of ^{222}Rn activity concentration and atmospheric pressure.

concentration could be explained by a pressure gradient from inside toward outside that leads to a leak of radon.

Without artificial aerosol production, the particle concentration was quite low in this house. Usually, it ranged between 500 and 5000 cm^{-3} with a mean particle concentration of 1200 cm^{-3}. This low particle concentration can be attributed to both the low air exchange rate, which does not bring particles from the outside, and the reduced human activity in the house. With aerosol sources such as cigar and cooking smokes, fumigating sticks (incense smoke), and burning candles, particle concentration highly increased to sometimes reach values around 1000000 cm^{-3}.

Unattached Fraction and Equilibrium Factor

With aged aerosol i.e., particle concentration between 500 and 5000 cm^{-3}, the unattached fraction of PAEC ranged between 0.08 and 0.67 with a mean value of 0.31 (Table 1), calculated from a series of 1000 data. The mean unattached fractions of ^{218}Po (f_{Po}) and ^{214}Pb (f_{Pb}) were equal to 0.69 and 0.23, respectively. Only 8% of the ^{214}Bi was found unattached. The mean value of f_p determined in the present study is high in comparison to most of the data reported in the literature and the value of 0.08 commonly used in dosimetric models. Indeed, the unattached fraction in indoor air is usually below 0.15 (Kojima and Abe 1988; Reineking and Porstendörfer 1990; Hopke et al. 1995). But one should note that in the places where these previous measurements had been carried out, the particle concentration was higher than in the dwelling mentioned above where the low particle concentration obviously explains the high f_p recorded. As a matter of fact our measurements gave a mean equilibrium factor of 0.16 (variation between 0.04 and 0.45), indicating an important disequilibrium between radon and its decay products. With a low particle concentration it is rare to have attachment, so radon decay products were mainly free and thus plated out on surfaces, leading to a small equilibrium factor. A typical example of the variations of the unattached fraction, equilibrium factor, and particle concentration is presented in Figure 6. For a particle concentration between 800 and 2800 cm^{-3}, f_p and F are in the ranges 0.14 – 0.43 and 0.15 – 0.34, respectively. This remarkably illustrates the inverse behavior of these two parameters. Moreover, it highlights that the amount of unattached fraction depends more on particle concentration than on the equilibrium factor.

Table 1
Mean, maximum, and minimum values of unattached fractions of PAEC, ^{218}Po, ^{214}Pb, and ^{214}Bi and equilibrium factor obtained with aged aerosol

	Mean	Maximum	Minimum
Equilibrium factor	0.16	0.45	0.04
Unattached fraction of PAEC	0.31	0.67	0.08
Unattached fraction of ^{218}Po	0.69	0.86	0.37
Unattached fraction of ^{214}Pb	0.23	0.61	0
Unattached fraction of ^{214}Bi	0.08	0.37	0

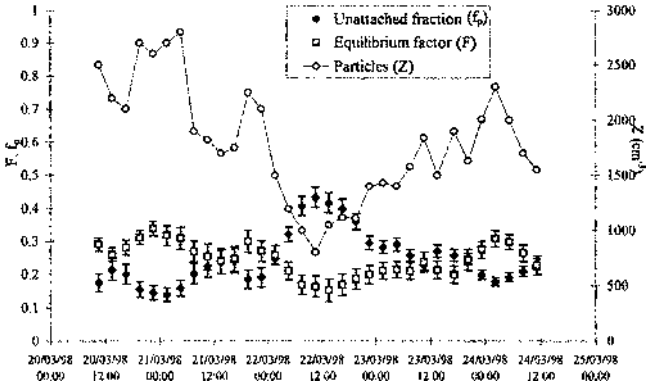

Figure 6. Variations of F, f_p, and Z with aged aerosol.

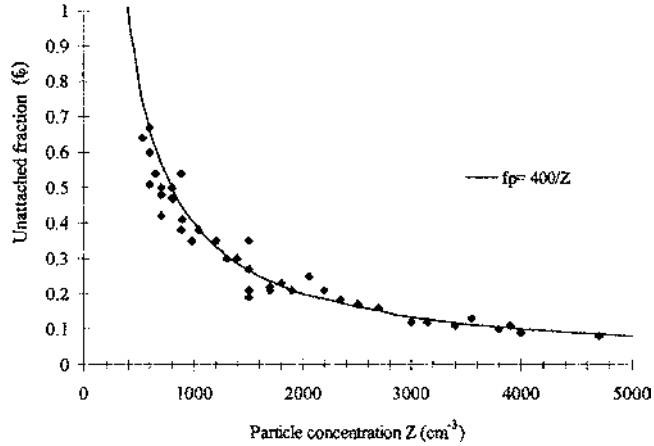

Figure 8. Unattached fraction of PAEC versus particle concentration.

However, our results concerning f_p were comparable to those found by Li and Hopke (1991) in indoor air and Cheng et al. (1997) in caverns, where particle concentrations were in the same range. A plot of the unattached fraction of ^{218}Po versus particle concentration (Figure 7), displaying their results and ours, showed a good agreement between all these measurements.

A deeper analysis of our f_p measurements with aged aerosol allowed us to establish the following relationship between the unattached fraction of PAEC and the particle concentration (Z), $f_p = 400/Z$; it is in agreement with previous suggestions by Porstendörfer (1996) (Figure 8). This curve shows that between 0 and 2000 cm^{-3} a small change in the particle concentration causes a high variation of unattached fraction. On the other hand, when the particle concentration is above 3000 cm^{-3}, the variations of the unattached fraction become negligible.

With aerosol sources, the unattached fraction became negligible (<5%) whereas the equilibrium factor was increased to sometimes reach 0.75 depending on the source used (Table 2). Under these conditions, there were nearly no unattached ^{214}Pb and ^{214}Bi, but there was some free ^{218}Po. Results analysis highlighted a possible distinction between the different aerosol sources: on the one hand, cooking activities and burning candles and on the other hand, cigar smoke and fumigating sticks. As a matter of fact, although cooking and candles produced a lot of particles, the equilibrium factor was comparable to the one found with aged aerosol when the particle concentration was around 5000 cm^{-3}. With cigar smoke and fumigating sticks, it reached higher values. These data therefore suggest that cooking and/or burning candles induce a production of particles in the nucleation mode where attachment is lower than in the accumulation mode. On the other hand, cigar and fumigating sticks would produce particles in the accumulation mode, leading to a greater attachment of nanometer radon decay products to these particles. These hypotheses were confirmed by the analysis of the number size distributions obtained through the combination of the diffusion battery and CNC. As illustrated in Figure 9, burning candles, like cooking, produced particles in the nucleation range, whereas those produced by cigar smoke and fumigating sticks were in the diameter range 160–200 nm. The influence of aerosol sources on the unattached fraction and equilibrium factor is illustrated in Figure 10.

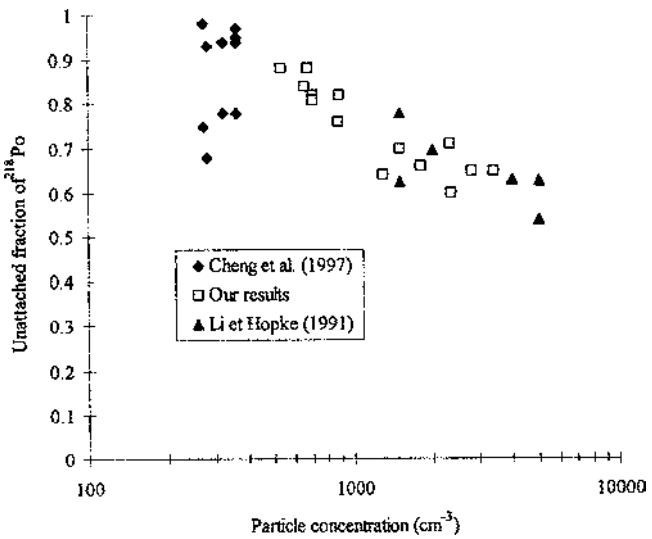

Figure 7. Comparison of unattached fraction of ^{218}Po versus particle concentration.

Finally, Figure 11 shows a plot of the unattached fraction versus the equilibrium factor with and without source. The continuous line corresponds to the correlation curve obtained between the two parameters mentioned above. One should note a low dispersion on both sides of the line. Since the formula $f_p = 0.0195 \times F^{-1.47}$ expresses the relationship between f_p and F, it can now be used as a calculation model for dwellings under typical domestic conditions. This formula was established from a large set of data covering the whole range of variations of the equilibrium factor (0.04–0.74) in opposition to the previous relationships established by Stranden and Strand (1986) and Tokonami et al. (1996), which were restricted to a small number of data and/or a short range of variations. Vargas et al. (2000) had previously obtained a similar relationship from measurements performed in several Spanish houses.

Table 2
Mean, maximum, and minimum values of particle concentration, unattached fractions of PAEC, ^{218}Po, ^{214}Pb, and ^{214}Bi, and equilibrium factor obtained with aerosol sources

	$Z \times 10^3$ cm^{-3}	Unattached fraction of PAEC	f_{Po}	f_{Pb}	f_{Bi}	Equilibrium factor
Cooking	250 (80–500)	0.046 (0.01–0.09)	0.18 (0.03–0.3)	0.017 (0–0.09)	0 (0–0.02)	0.27 (0.15–0.4)
Fumigating sticks	100 (60–450)	0.02 (0.01–0.05)	0.069 (0.047–0.17)	0.017 (0–0.075)	0	0.49 (0.3–0.59)
Burning candles	390 (100–1,000)	0.032 (0.022–0.047)	0.10 (0.01–0.16)	0.023 (0.014–0.06)	0	0.31 (0.26–0.35)
Cigar smoke	80 (60–300)	0.024 (0.012–0.039)	0.10 (0.07–0.15)	0.001 (0–0.007)	0.001 (0–0.007)	0.56 (0.26–0.74)

MODEL-EXPERIMENT COMPARISON

Field measurements and physical process modeling constitute two complementary approaches to study the behavior of radon decay products in indoor air. Unfortunately only few theory-experiment comparisons have been performed to check models. The PRADDO model (Gouronnec 1995), an extension of the room model (Jacobi 1972; Porstendörfer et al. 1978), has already been tested in a town hall basement with a high particle concentration (Gouronnec et al. 1996). But this model was not validated for the nanometer radon decay products. That is why we tried to check performance of the PRADDO model under conditions of low ambient aerosol particle concentration.

For this purpose, the time period shown in Figure 6 was examined. The model input data were either field measurements (radon activity concentration, attachment rate, ventilation rate) or literature data (recoil probability of ^{218}Po, free and attached deposition rates, radioactive decay constants). Using the attachment theory we determined the attachment rates from the number size distributions obtained, as previously mentioned. Table 3 gives the values of the input data used in our calculations for the period of concern; the variations of attachment rate and radon activity concentration are depicted in Figure 12. Free and attached deposition rates were set at 20 and 0.2 h^{-1}, respectively, these values being recommended by Knutson (1988) for indoor conditions. Following the hypotheses of a permanent regime and homogeneous atmosphere, the differential equations taking into account radioactive decay, deposition, attachment, recoil, and ventilation processes were solved; new values of unattached, attached, and deposited activity concentrations for each radon decay product, potential alpha energy concentration, unattached fraction, and equilibrium factor were then obtained and compared to the corresponding experimental ones.

The results dealing with total, attached, and free PAEC are depicted in Figure 13. During the analyzed period of time, the total measured PAEC ranged between 1.5 and 2.8 μJ m^{-3}. One should notice, first, that the calculated values follow the variations of the experimental data. The model is thus capable of reproducing the changes in ambient conditions due to variations of radon activity concentration and/or particle concentration. It

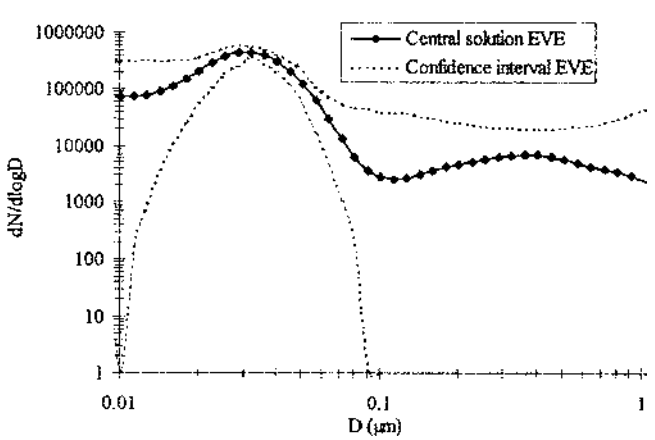

Figure 9. Example of number size distribution obtained with burning candles.

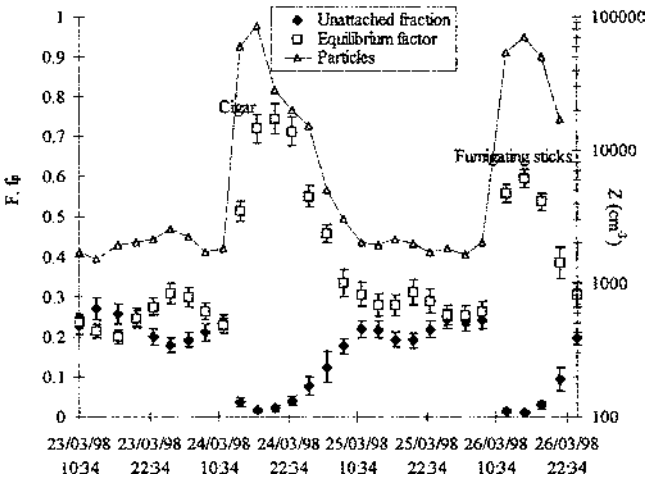

Figure 10. Variation of F, f_p, and Z with aerosol sources.

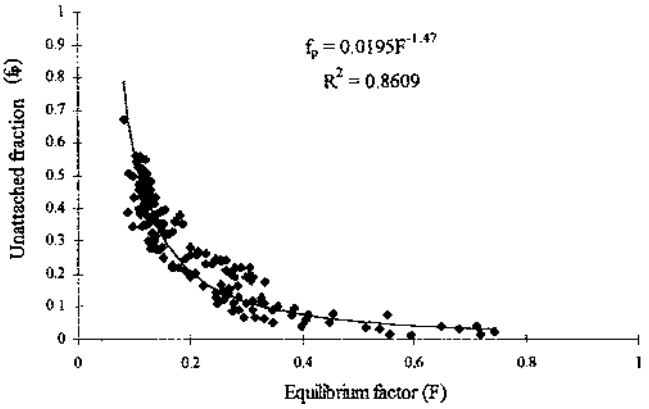

Figure 11. Unattached fraction versus equilibrium factor under domestic conditions.

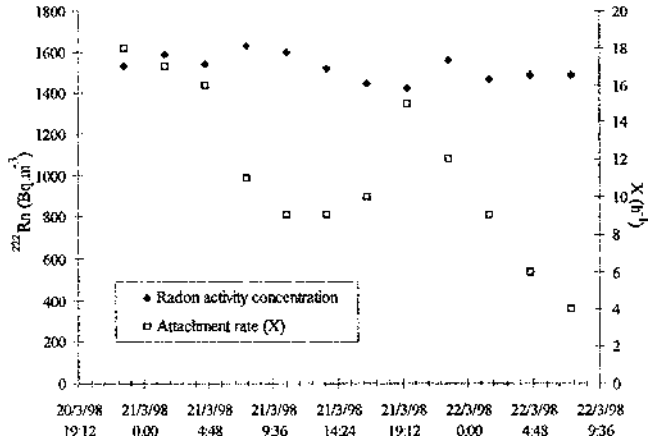

Figure 12. Variation of ^{222}Rn activity concentration and attachment rate during the examined period.

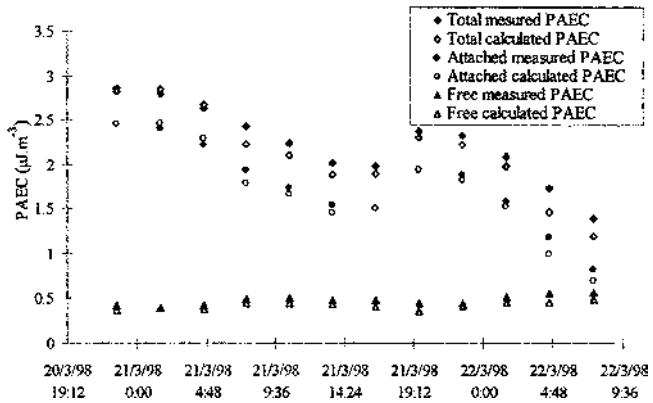

Figure 13. Model-experiment comparison for total, attached, and free PAEC with aged aerosol.

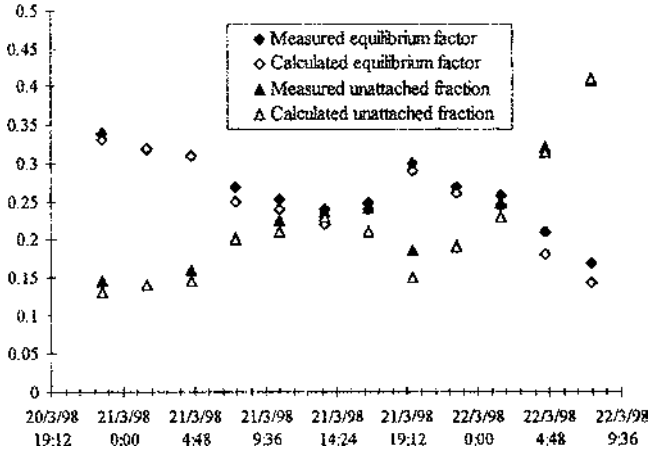

Figure 14. Model-experiment comparison for unattached fraction and equilibrium factor with aged aerosol.

appears also that the input values of 20 and 0.2 h^{-1}, respectively, for free and attached deposition rates are representative of the considered dwelling. Moreover, there is a good agreement between the two types of values with a mean deviation of, respectively, 6, 5, and 11% for total, attached, and unattached PAEC. As a consequence, the agreement for unattached fraction and equilibrium factor is also quite satisfactory, as illustrated in Figure 14. The mean deviation of experimental results from theoretical data for the unattached fraction and the equilibrium factor was 6 and 5.5%, respectively.

It is then obvious that, with an aged aerosol, the PRADDO model faithfully reproduced our experimental results and demonstrated its capability to satisfactorily describe the behavior of nanometer radon decay products.

In a second step, the model was tested under all the conditions investigated in the dwelling, i.e., with and without sources. So 27 situations covering the whole range of variations observed for unattached fraction and equilibrium factor were extracted from our database. (i) Free and attached deposition rates and recoil probability of ^{218}Po were identical to the values previously taken. (ii) Ventilation rate was either 0.2 or 0.25 h^{-1}. (iii) Attachment rate and radon activity concentration ranged between 930 and 1.5 h^{-1} and 400 and 1800 Bq m^{-3}, respectively, as illustrated in Figure 15.

The results of the model-experiment comparison for total activity concentration of ^{218}Po, ^{214}Pb, and ^{214}Bi are depicted in

Table 3
Input values of the PRADDO model with aged aerosol

Parameter	Value
^{222}Rn activity concentration	Figure 12
Ventilation rate	0.15 h^{-1}
Free deposition rate	20 h^{-1}
Attached deposition rate	0.2 h^{-1}
Recoil probability of ^{218}Po	0.83
Attachment rate	Figure 12

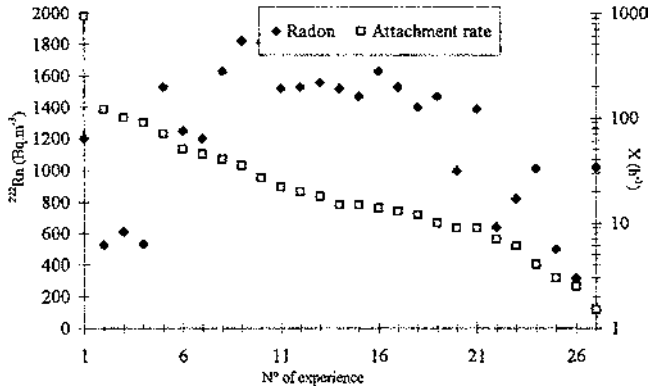

Figure 15. Variations of ^{222}Rn activity concentration and attachment rate for the 27 situations examined.

Figures 16, 17, and 18, respectively. For the three radon decay products, there is good agreement between the calculated and experimental data. However, the values calculated for ^{218}Po are greater than the experimental data, with a mean deviation of 9.4% for a range of variations between 0.4 and 32%. The most significant deviations were obtained with high particle concentration, especially under cooking conditions. For ^{214}Pb, the calculated values were usually equal or below the experimental ones. The mean deviation was 10.7% for a variation range within 0 and 52%. ^{214}Bi had the same behavior as the one observed for ^{214}Pb, which means that the PRADDO model tends to underestimate the experimental data; there was a mean deviation of 13.4% between experimental and calculated values. Finally, the results dealing with equilibrium factor are given in Figure 19. For the 27 experiments analyzed, it ranged between 0.08 and 0.75. A very good agreement was observed

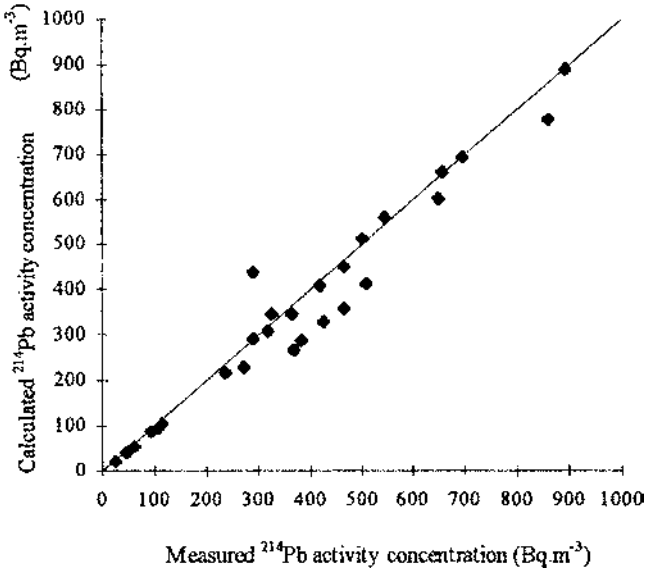

Figure 17. Model-experiment comparison for total ^{214}Pb activity concentration.

and the mean deviation was 6% for a variation within 0 and 21%.

On the whole, satisfactory results between calculated and experimental values under different aerosol conditions were obtained. Input parameters, particularly those taken from the literature, seem to be representative of the conditions of the dwelling of concern. Nevertheless, overestimation of total ^{218}Po activity concentration could be explained by an underestimation of the free deposition rate with aerosol sources, which will confirm the observations made by Porstendörfer et al. (1987) and Li and

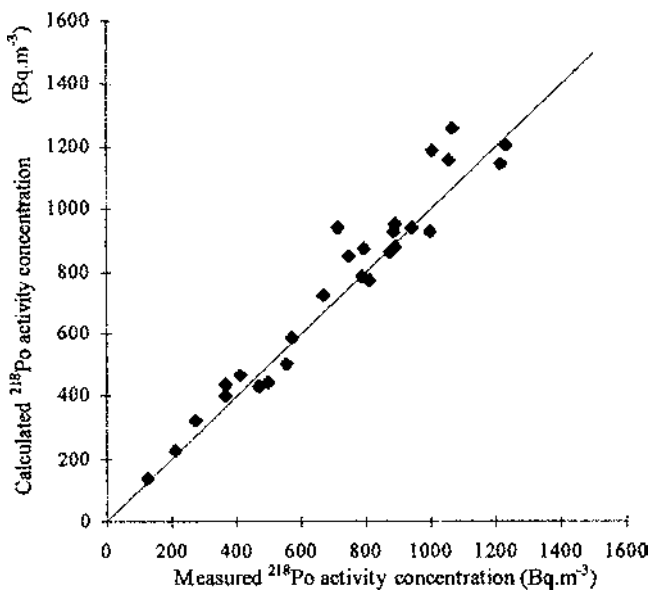

Figure 16. Model-experiment comparison for total ^{218}Po activity concentration.

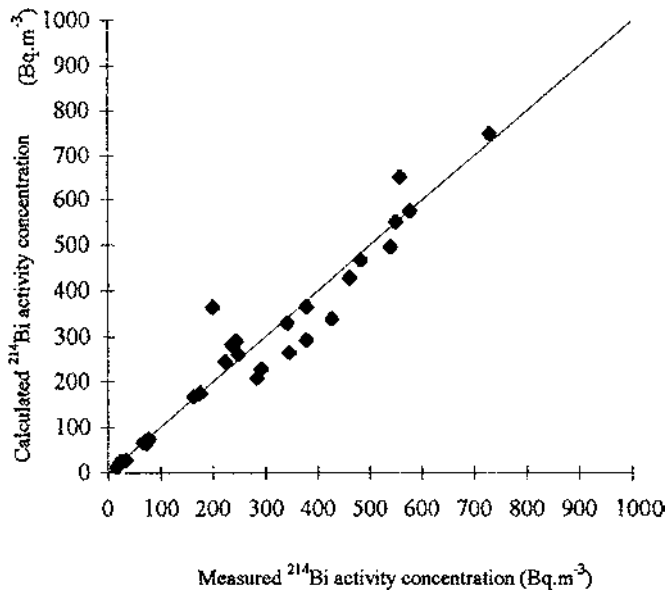

Figure 18. Model-experiment comparison for total ^{214}Bi activity concentration.

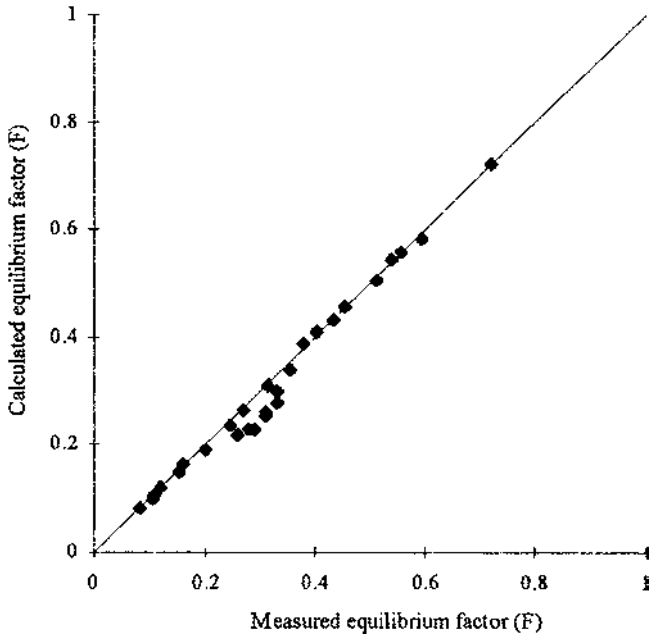

Figure 19. Model-experiment comparison for equilibrium factor.

Hopke (1991). It is indeed likely that the presence of organic compounds will entail a greater neutralization of nanometer radon decay products, resulting in a more important diffusion.

CONCLUSION

To carry out measurements of equilibrium factor and unattached fraction over 1 y in a house under realistic living conditions, an original device was developed and implemented; it was composed of an annular diffusion channel set in parallel with an open filter. An important set of data was recorded, and investigations dealt in particular with the temporal variability of unattached fraction and equilibrium factor. The correlation relationship established between these two parameters over this study can now be used as a calculation model for dwellings under domestic conditions. All of the data presented above were recently used by Marsh and Birchall (Monchaux 1999) to perform an uncertainty analysis. It permitted them to determine the probability distributions of the physical parameters, such as equilibrium factor and unattached fraction, and thus estimate the uncertainty in the effective dose per unit exposure to radon.

The comparison of our experimental data with the theoretical values calculated from PRADDO model highlighted the following points. (i) With aged aerosol, a good agreement was found between calculated and experimental activity concentrations of each radon decay product, PAEC, equilibrium factor, and unattached fraction; it consequently permitted us to evaluate the model ability to describe the behavior of nanometer radon decay products. (ii) Satisfactory results were also obtained between model and experiments with the different aerosol sources investigated. Finally, it nevertheless seems that the free deposition rate with aerosol sources may be higher than the value of 20 h^{-1} recommended by Knutson. However, the PRADDO model is a good alternative to long-term measurements to calculate the exposure required to assess the dose received by the general population from input data like radon concentration, particle concentration and size, and ventilation rate.

ACKNOWLEDGMENTS

This work was partially funded by the European Union under contract FI4P-CT95-0025. We wish to thank Dr. Friocourt for her assistance in the writing of an English manuscript.

REFERENCES

Birchall, A., and James, A. C. (1994). Uncertainty Analysis of the Effective Dose per Unit Exposure from Radon Progeny and Implications for ICRP Risk-Weighting Factors, *Radiat. Prot. Dosim.* 53:S133–S140.

CEC Report. (1998). *Risk Assessment of Exposure to Radon Decay Products*, Progress Report, Contract FI4P-CT-95-0025.

Cheng, Y. S., Chen, T. R., Wasiolek, P., and Van Engen, A. (1997). Radon and Radon Progeny in the Carlsbad Caverns, *Aerosol Sci. Technol.* 26:74–92.

Genrich, V. (1994). *Report*, Genitron Instruments, Frankfurt, Germany.

Gouronnec, A. M. (1995). Modélisation et étude expérimentale du comportement du Radon et de ses descendant s dans une enceinte confinée. Application à une habitation, Ph.D. thesis, University of Paris XII.

Gouronnec A. M., Goutelard, F., Montassier N., Boulaud D., Renoux A., and Tymen, G. (1996). Behavior of Radon and its Daughters in a Basement: Model-Experiment Comparison, *Aerosol Sci. Technol.* 25:73–89.

Grimsrud, D. T., Sherman, M. H., and Sonderegger, R. C. (1983). *ASHRAE Conference Thermal Performance of Exterior Envelopes of Buildings*, Las Vegas, NV.

Grot, R. A., and Clark, R. E. (1981). *ASHRAE Conference Thermal Performance of Exterior Envelopes of Buildings*, Orlando, FL.

Hopke, P. K., Jensen B., Li, C. S., Montassier, N., Wasiolek, P., Cavallo, A., Gatsby, K., Socolow, R., and James, A. C. (1995). Assessment of the Exposure to and Dose from Radon Decay Products in Normally Occupied Homes, *Environ. Sci. Technol.* 19:1359–1364.

Huet, C. (1999). Etude des caractéristiques physiques-distributio n en taille, fraction libre, fraction d'équilibre-des dé rivés d viecourte du Rn222 en atmosphere domestique. Ph.D. thesis, University of Brest.

Jacobi, W. (1972). Activity and Potential Alpha-Energy of Rn-222 and Rn-220 Daughters and their Decay Products in the Atmosphere, *J. Geophys. Res.* 68:3799.

James, A. C., Bradford, G. F., and Howell, D. M. (1972). Collection of Unattached RaA Atoms using a Wire Gauze, *J. Aerosol Sci.* 3:243–250.

Kerouanton, D. (1996). Etude de la composante ultrafine issue du Radon-222 à partir d'un canal de diffusion annulaire muni d'un dètecteur solide de traces nucléaires, Ph.D. thesis, University of Brest.

Kerouanton, D., Tymen, G., and Boulaud, D. (1996). Small Particle Diffusion Penetration of an Annular Duct Compared to Other Geometries, *J. Aerosol Sci.* 27:345–349.

Knutson, E. O. (1988). Modeling Indoor Concentrations of Radon's Decay Products, In *Radon and its Decay Products in Indoor Air*, edited by W. W. Nazaroff, and A. V. Nero, John Wiley and Sons, New York, pp. 161–202.

Knutson, E. O., and George, A. C. (1994). Measurements of ^{214}Pb Loss by Recoil from Decay of ^{218}Po Collected on a Wire Screen, *J. Aerosol Sci.* 25: S71–S72.

Kojima, H., and Abe, S. (1988). Measurements of the Total and Unattached Radon Daughters in a House, *Radiat. Prot. Dosim.* 24:241–244.

Li, C. S., and Hopke, P. K. (1991). Efficacy of Air Cleaning Systems in Controlling Indoor Radon Decay Products, *Health Physics* 61:785–797.

Lubin, J. H., Tomasek, L., Edling, C., Hrnung, R. W., Howe, J., Kunz, E., Kusiak, R. A., Morrison, H. I., Radford, E. P., Samet, J. M., Tirmarche, M., Woodward, A., Xiang, Y. S., and Pierce, D. (1994). *Radon and Lung Cancer Risk: A Joint Analysis of 11 Underground Miner Studies*, NIH Publication no. 94-3644.

Marsh, J., and Birchall, A. (1998). Sensivity Analysis of the weighted Equivalent Lung Dose per Unit Exposure from Radon Progeny. Memorandom NRPB-M915. NRPB, Chilton, Didcot, Oxfordshire, OX11 ORQ, UK.

Mercer, T. T., and Mercer, R. (1970). Diffusional Deposition from a Fluid Flowing Radially Between Concentric, Parallel, Circular Plates, *J. Aerosol Sci.* 1:279–285.

Monchaux, G. (1999). *Risk Assessment of Exposure to Radon Decay Products*, RARAD final report, report CEA-R 5882(E). Edited by La Direction de l'Information Scientifique et Technique, CEA Saclay 91191 Gif-sur-yvette Cedex France.

Paatero, P. (1990). The Extreme Value Estimation Deconvolution Method with Application to Aerosol Research, University of Helsinki, Report series in Physics, HU-P-250.

Porstendörfer, J. (1996). Radon: Measurements Related to Dose, *Environ. Inter.* 22:563–583.

Porstendörfer, J., Reineking, A., and Becker, K. H. (1987), Free Fractions, Attachment Rates and Plateout Rates of Radon Daughters in Houses. In *Radon and its Decay Products—Occurrence, Properties, and Health Effects*. American Chemical Society, pp. 285–300.

Porstendörfer, J., Wicke, A., and Scraub, A. (1978). The Influence of Exhalation, Ventilation and Deposition Process Upon the Concentration of Radon-222 and Radon-220 and Their Decay Products in Room Air, *Health Physics* 34:465–473.

Porstendörfer, J., Wicke, A., and Schraub, A. (1980). Methods for Continuous Registration of Radon, Thoron, and Their Decay Products Indoors and Outdoors. In *Natural Radiation Environment III*. US Department of Energy, Washington D.C., CONF-780422, 2:1293–1307.

Ramamurthi, M., and Hopke, P. K. (1989). On Improving the Validity of Wire Screen "Unattached" Fraction Radon Daughter Measurements, *Health Physics* 56:189–194.

Reineking, A., Butterweck, G., Kesten, J., and Porstendörfer, J. (1990). *29th Hanford Symposium on Health and the Environment*, Richland, USA, 15–19 October.

Reineking, A., and Porstendörfer, J. (1990). "Unattached" Fraction of Short-Lived Rn Decay Products in Indoor and Outdoor Environments: An Improved Single-Screen Method and Results, *Health Physics* 58:715–727.

Stranden, E., and Berteig, L. (1982). Radon Daughter Equilibrium and Unattached Fraction in Mine Atmospheres, *Health Physics* 42:479–487.

Stranden, E., and Strand, T. (1986). A Dosimetric Discussion Based on Measurements of Radon Daughter Equilibrium and Unattached Fraction in Different Atmospheres, *Radiat. Prot. Dosim.* 16:313–318.

Tapper, U. (1995). Solution of Linear Inversion Problems and Factor Analytic Problems with Matrix Based Models, Ph.D. thesis, University of Helsinki.

Tokonami, S., Iimoto, T., and Kurosawa, R. (1996). Continuous Measurement of the Equilibrium Factor F and the Unattached Fraction f_p of Radon Progeny in the Environment, *Environ. Inter.* 22:S611–S616.

Tremblay, R. J., Leclerc, A., Mathieu, C., Pepin, R., and Townsend, M. G. (1979). Measurement of Radon Progeny Concentration in Air by α-Particle Spectrometric Counting During and After Air Sampling, *Health Physics* 36:401–411.

Tymen, G., Kerouanton, D., Huet, C., and Boulaud, D. (1999). An Annular Diffusion Channel Equipped with a Track Detector Film for Long-Term Measurements of Activity Concentration and Size Distribution of ^{218}Po Particles, *J. Aerosol Sci.* 30:205–216.

UNSCEAR. (1993). *Ionising Radiation: Sources and Biological Effects*, United Nations, New York.

Vargas, A., Ortega, X., and Porta, M. (2000). Dose Convenion Factor for Radon Concentration in Indoor Environments Using a New Equation for the F-fp Correlation. *Health Physics* 78(1):80–85.